Efficient Representation of Spectral BRDFs

Huiying Xu and Yinlong Sun
Department of Computer Sciences, Purdue University
W. Lafayette, Indiana, USA

Abstract

We propose a hybrid method to efficiently represent spectral BRDFs. We first perform Fourier transform to the spectrum for given incident and outgoing directions, and then decompose the Fourier coefficients into a smooth background and a sharp peak. The smooth background will be represented with a linear combination of spherical harmonics, and the sharp peak with a Gaussian function. The errors of representation are studied. This method has a potential of applications in color synthesis and analysis.

1. Introduction

In color image synthesis and analysis, a fundamental problem is to accurately characterize light scattering from objects. This behavior is generally described by a *bi-directional scattering distribution function* (BSDF)[1]

$$\rho(\theta_i,\varphi_i,\theta_o,\varphi_o,\lambda)=\frac{dL_o(\theta_o,\varphi_o,\lambda)}{L_i(\theta_i,\varphi_i,\lambda)\cos\theta_i d\Omega_i}\ , \qquad (1)$$

which is the ratio between the scattered radiance and incident irradiance, where (θ_i,φ_i) and (θ_o,φ_o) specify the incident (lighting) and outgoing (viewing) directions (Figure 1), and λ is wavelength. In case of reflection and transmission at a surface, a BSDF becomes respectively a *bi-directional reflection distribution function* (BRDF) and *bi-directional transmission distribution function* (BTDF). This paper focuses on BRDFs, but the proposed method is inherently applicable to BSDFs and BTDFs.

A number of analytic studies[2-8] have been conducted to model surface reflection behavior. However, the existing methods still need to improve in accuracy and generality. The key challenge roots in the tremendous complexity of surface reflection process. This process may involve not only the incident and outgoing directions, wavelength, and polarization, but also surface properties such as roughness and anisotropy, bulk material properties such as volume absorptivity, and multiple scattering.[9]

Alternatively, one may obtain BRDFs from experimental measurements or numerical simulations. A common strategy is to sample a BRDF in each dimension, including four angles and wavelength (or color components). However, this requires a huge data size in representation. Another strategy represents a BRDF directly with a linear combination of basis functions such as spherical harmonics[10,13] and wavelets.[13,15] However, when a BRDF has a sensitive dependency on directions, a large number of coefficients might be needed. Recently, a factored representation[16-18] was proposed by factoring a BRDF into the product of low-dimensional functions. Following this idea, a method based on importance has also been developed to improve the storage efficiency of BRDFs.[19]

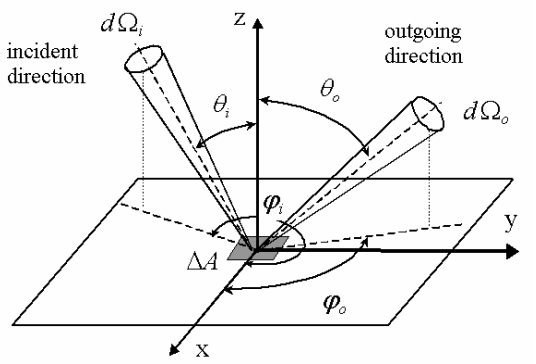

Figure 1. The geometry and notations of surface scattering.

These previous studies have focused on RGB-based BRDFs. However, it has been shown that the RGB-based approach is inadequate for faithful color imaging and that spectral information is necessary.[20-23] For example, wavelength information is necessary for rendering light interference or diffraction. This motivates the current work.

In the past,[24] we proposed to represent spectral BRDFs by performing Fourier transform to the spectra of all incident and outgoing directions, and then express the same-order Fourier coefficients by a linear combination of spherical harmonics. However, that approach is still not efficient enough for those BRDFs that have a sensitive dependency on directions.

In this paper, we propose a hybrid method to represent spectral BRDFs compactly. We first perform the Fourier transform to the spectrum for each combination of the incident and outgoing directions. Then, for each incident direction, we decompose the same-order Fourier coefficients of spectra into a smooth background and a sharp peak (which has a sensitive angular dependency). Since the smooth background is dominated by low-frequency components, we propose to represent the smooth background using a linear

combination of low-level spherical harmonics. On the other hand, the sharp peak contains significant high-frequency components and we represent it with a Gaussian function. We have conducted numerical studies of the representation errors using this hybrid method, and the results show that it has significantly improved the representation efficiency of spectral BRDFs.

2. Representation of Spectral BRDFs

2.1 Fourier Transform

A BRDF function can generally be decomposed into the diffuse and specular components

$$\rho(\theta_i,\varphi_i,\theta_o,\varphi_o,\lambda) = \rho_{diffuse}(\theta_i,\varphi_i,\theta_o,\varphi_o,\lambda) + \rho_{specular}(\theta_i,\varphi_i,\theta_o,\varphi_o,\lambda) \quad . \tag{2}$$

Typically, the specular component has a lobe that depends sensitively on the outgoing direction and has the maximum at a specific direction. For convenience in this paper, we call this direction "mirror-reflection direction", although the true mirror-reflection direction does not always generate the maximum (see Ref. [3]). In contrast, the diffuse component is insensitive to the outgoing direction.

Furthermore, we assume that both diffuse and specular components could be expressed in terms of a product of an angle-dependent geometric factor and a wavelength-dependent factor. That is,

$$\rho(\theta_i,\varphi_i,\theta_o,\varphi_o,\lambda) = G_{diffuse}(\theta_i,\varphi_i,\theta_o,\varphi_o)C_{diffuse}(\lambda) + G_{specular}(\theta_i,\varphi_i,\theta_o,\varphi_o)C_{specular}(\lambda) \tag{3}$$

The consideration here is that all physical surfaces can be classified into two categories. In the first category, a surface is a simple interface that separates the material from its environment, and the material is homogeneous across the surface. Common examples are metallic surfaces. In this case, since the wavelength dependencies of the diffuse and specular components are caused by the same material, the diffuse and specular colors are similar. In the second category, a physical surface consists of two or more layers. Examples include painted or varnished surfaces such as skins and automobiles. In this case, the specular component is mainly associated with the top layer, and the diffuse component involves both the top and sub-layers. Therefore, the diffuse and specular colors might be very different. A good example is painted wood furniture, where the specular color is white (the color of illuminating light) while the diffuse color is dominated by the color of wood.

Given a spectral BRDF, we first perform a Fourier transform in the wavelength dimension:

$$\rho(\theta_i,\varphi_i,\theta_o,\varphi_o,\lambda) = \frac{1}{2}a_0(\theta_i,\varphi_i,\theta_o,\varphi_o) + \sum_{k=1}\left\{a_k(\theta_i,\varphi_i,\theta_o,\varphi_o)\cos\left[\frac{2\pi k(\lambda-\lambda_{\min})}{\Delta\lambda}\right] + b_k(\theta_i,\varphi_i,\theta_o,\varphi_o)\sin\left[\frac{2\pi k(\lambda-\lambda_{\min})}{\Delta\lambda}\right]\right\}, \tag{4}$$

where $\Delta\lambda = \lambda_{\max} - \lambda_{\min}$ is the visible range, and

$$a_k(\theta_i,\varphi_i,\theta_o,\varphi_o) = \frac{2}{L}\int_{\lambda_{\min}}^{\lambda_{\max}} d\lambda\rho(\theta_i,\varphi_i,\theta_o,\varphi_o,\lambda)\cos\left[\frac{2\pi k(\lambda-\lambda_{\min})}{\Delta\lambda}\right], \quad k=0,1,\ldots,\infty,$$
$$b_k(\theta_i,\varphi_i,\theta_o,\varphi_o) = \frac{2}{L}\int_{\lambda_{\min}}^{\lambda_{\max}} d\lambda\rho(\theta_i,\varphi_i,\theta_o,\varphi_o,\lambda)\sin\left[\frac{2\pi k(\lambda-\lambda_{\min})}{\Delta\lambda}\right], \quad k=1,2,\ldots,\infty. \tag{5}$$

Substituting Eq. (3) into (5), we can express the Fourier coefficients as

$$\mathfrak{F}_\lambda\left[\rho(\theta_i,\varphi_i,\theta_o,\varphi_o,\lambda)\right](k) = G_{diffuse}(\theta_i,\varphi_i,\theta_o,\varphi_o)\mathfrak{F}_\lambda\left[C_{diffuse}(\lambda)\right](k) + G_{specular}(\theta_i,\varphi_i,\theta_o,\varphi_o)\mathfrak{F}_\lambda\left[C_{specular}(\lambda)\right](k) \quad , \tag{6}$$

where $\mathfrak{F}_\lambda\left[\rho(\theta_i,\varphi_i,\theta_o,\varphi_o,\lambda)\right](k)$ represents Fourier coefficients $a_k(\theta_i,\varphi_i,\theta_o,\varphi_o)$ or $b_k(\theta_i,\varphi_i,\theta_o,\varphi_o)$.

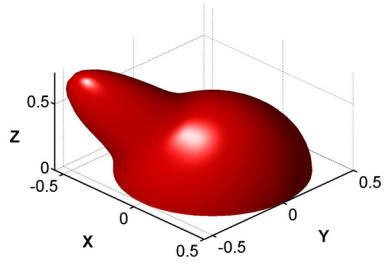

(a)

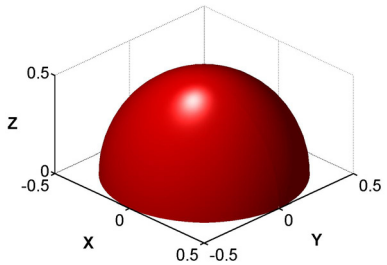

(b)

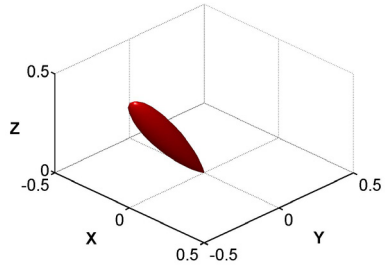

(c)

Figure 2. Decomposition of spatial distribution of a Fourier coefficient (a) into a smooth background (b) and a sharp peak (c).

2.2 Spherical Harmonics and Gaussian Function

Since each Fourier coefficient is a bi-directional function that depends on the incident and outgoing

directions, we can express it using a linear combination of spherical harmonics. However, if we attempt to represent the Fourier coefficient directly using the spherical harmonics, the representation would not be efficient when the coefficient has a sensitive angular dependency, which is associated with the specular term. Based on this consideration, we propose to decompose the same-order Fourier coefficients into a smooth background and a super-imposed sharp peak. Since the smooth background mainly contains low-frequency components, it can be represented well with a linear combination of low-level spherical harmonics. On the other hand, the sharp peak can be described by a Gaussian function conveniently. Figure 2 illustrates this approach, where Fourier coefficients of the same order are decomposed into a smooth background and a sharp peak.

Thus, continuing from Eq. (6),

$$\mathcal{F}_\lambda\left[\rho(\theta_i,\varphi_i,\theta_o,\varphi_o,\lambda)\right](k)=\sum_{l=0}^{L}\sum_{m=-l}^{l}A_{k,\,(l,m)}(\theta_i,\varphi_i)Y_{l,m}(\theta_o,\varphi_o) + p_k\exp[-\alpha_k^2/b_k] \quad , \quad (7)$$

where $Y_{l,m}(\theta_o,\varphi_o)$ is the spherical harmonic function of level l and order m, L is the maximum level of spherical harmonics used for the representation, $A_{k,\,(l,m)}(\theta_i,\phi_i)$ are the coefficients, and p_k and b_k specify the height and width of the separated peak. Note that α_k is the angle between the outgoing direction (θ_o , φ_o) and the mirror-reflection direction (θ_p , φ_p) at which the peak is maximal.

2.3 Decomposition of Fourier Coefficients

Before decomposing the Fourier coefficients, we need to identify the mirror-reflection direction (θ_p , φ_p). In principle, this direction can be determined using numerical calculation such as regression analysis.[25] Considering that the specular part (the second term in Eq. (6)) near the mirror-reflection direction is remarkably larger than the diffuse part (the first term in Eq. (6)), we will use Gaussian function for the regression analysis.

First, we consider the 1D case and a generic Gaussian

$$f(\alpha)=\exp[A+B\alpha+C\alpha^2] \quad , \quad (8)$$

where A, B, and C are coefficients to be determined. Since

$$\exp[A+B\alpha+C\alpha^2]=\exp\left\{C\left[(\alpha+\frac{B}{2C})^2-\frac{B^2}{4C^2}+\frac{A}{C}\right]\right\} \quad , \quad (9)$$

$\alpha=-B/(2C)$ gives the center of the peak. The regression analysis to determine the coefficients can be expressed as

$$\Omega=\sum_m\left\{\ln f(\alpha_m)-\ln f_m\right\}^2=\sum_m\left\{A+B\alpha_m+C\alpha_m^2-\ln f_m\right\}^2$$
$$\frac{\partial\Omega}{\partial A}=0,\ \ \frac{\partial\Omega}{\partial B}=0,\ \ \frac{\partial\Omega}{\partial C}=0 \quad (10)$$

This equation can be transformed into

$$\begin{aligned} A\sum 1+B\sum_m\alpha_m+C\sum_m\alpha_m^2&=\sum_m\ln f_m,\\ A\sum_m\alpha_m+B\sum_m\alpha_m^2+C\sum_m\alpha_m^3&=\sum_m\alpha_m\ln f_m,\\ A\sum_m\alpha_m^2+B\sum_m\alpha_m^3+C\sum_m\alpha_m^4&=\sum_m\alpha_m^2\ln f_m. \end{aligned} \quad (11)$$

The procedure is similar for 2D case, in which the outgoing directions (θ_o,φ_o) are regularly distributed. The algorithm for finding (θ_p , φ_p) is summarized below:

1. Find all outgoing directions (θ_o,φ_o) in which the BRDF values are remarkably larger than those of other outgoing directions.
2. For each group of (θ_o,φ_o) with respect to each value of θ_o , use the regression analysis in Eqs. (8-11) to find the center of the peak, and store it into array Y.
3. For each group of (θ_o,φ_o) with respect to each value of φ_o , use the regression analysis Eqs. (8-11) to find the center of the peak, and store it into the array X.
4. Calculate the average value in array X and set it as θ_p , and then calculate the average value in array Y and set it as φ_p .

The decomposition of the sharp peak from the smooth background is the key point for our hybrid representation method. For this purpose, we need to set a critical angle first. For any outgoing directions with angle from the mirror-reflection direction larger than the critical angle, we will regard them as being part of the smooth background. Then we use the regression analysis to determine coefficients $A_{k,\,(l,m)}(\theta_i,\phi_i)$. The expressions are:

$$\Omega=\sum_v\left\{\mathcal{F}_\lambda\left[\rho(\theta_i,\phi_i,\theta_o,\phi_o,\lambda)\right](k)-\sum_{l=0}^{L}\sum_{m=-l}^{l}A_{k,\,(l,m)}(\theta_i,\phi_i)Y_{l,m}(\theta_o,\phi_o)\right\}^2 ,$$
$$\frac{\partial\Omega}{\partial A_{k,\,(l,m)}(\theta_i,\phi_i)}=0 \ . \quad (12)$$

Eq. (12) can be transformed into a series of linear equations

$$\sum_{l,m}A_{k,\,(l,m)}(\theta_i,\phi_i)\sum_v Y_{l,m}(\theta_o,\phi_o)Y_{l',m'}(\theta_o,\phi_o) = \sum_v\mathcal{F}_\lambda\left[\rho(\theta_i,\phi_i,\theta_o,\phi_o,\lambda)\right](\lambda)\ Y_{l',m'}(\theta_o,\phi_o) \quad , \quad (13)$$

where $l'=0,\ 1,\ 2,\ ...,\ L$, and $-l'\le m'\le l'$. Solving these linear equations in Eq. (13), the coefficients $A_{k,\,(l,m)}(\theta_i,\phi_i)$ can be obtained.

Having obtained the coefficients $A_{k,\,(l,m)}(\theta_i,\phi_i)$, we can extract the smooth background first. Then we follow the regression analysis in Eqs. (8-11) to determine coefficients p_k , b_k and α_k . Since the mirror-reflection direction (θ_p , φ_p) has been obtained, we can conveniently calculate the angle between any outgoing direction and the mirror-reflection direction.

3. Numerical Studies

To verify the efficiency and accuracy of our method, we apply it to representing BRDFs that are generated using the Phong illumination model[4,26]:

$$I = I_1(\lambda)[k_d S_d(\lambda)(\vec{I}\cdot\vec{N}) + k_s S_s(\lambda)(\vec{R}\cdot\vec{N})^n] \ , \qquad (14)$$

where I is the reflected light intensity, I_1 is the light intensity of a point source, n is positive integer (the Phong power), $\vec{I}$, $\vec{N}$ and $\vec{R}$ denote the directions of the incident light, surface normal, and reflected light, respectively, and k_d and k_s are the diffuse and specular coefficients. $S_d(\lambda)$ and $S_s(\lambda)$ correspond to spectral reflectances for the diffuse and specular terms. In our numerical study, the spectra $S_d(\lambda)$ and $S_s(\lambda)$ are taken from those of the Green and White in Macbeth Color Checkers[1] (see Figure 3).

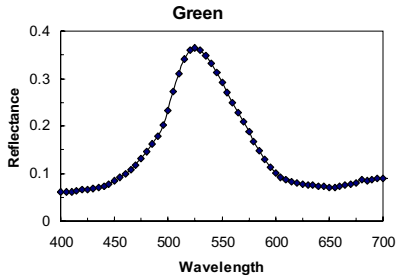

(a)

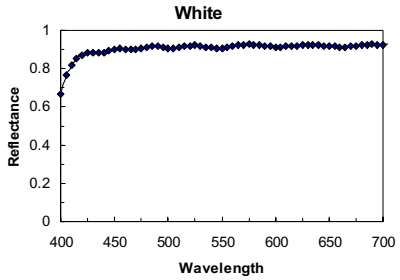

(b)

Figure 3. Spectra of Green (a) and White (b) in Macbeth Color Checkers.

First, for the purpose of comparison, we represent the same-order Fourier coefficients directly using a linear combination of spherical harmonics without decomposing them into a smooth background and a sharp peak. For all the sampled outgoing directions, the total relative error between the representation and generated BRDFs versus k_s/k_d and the Phong power n is shown in Figure 4. Here, the incident direction is $\theta_i = 15$, $\varphi_i = 0$, the maximum level of spherical harmonics is $L = 4$, and 13 Fourier coefficients are used. (Below all Fourier transforms use 13 coefficients).

Since we use the Phong model to generate spectral BRDFs, the relative height of peak to the smooth background in Fourier coefficients increases with the value of k_s/k_d, and the width of peak decreases with n. Therefore, both increases in k_s/k_d and n will result in the change of BRDF shape from being smooth to having a sharp peak. In Figure 4, we can see that, for a fixed Phong power n, the relative error increases with k_s/k_d. However, for a fixed k_s/k_d, the relative error decreases first, then increases quickly with n. This behavior is caused by the fact that we use the maximum level of spherical harmonics $L = 4$. Large L increases the ability of linear combination of spherical harmonics to represent the functions with complicated geometrical shape, and a small change in geometrical shape from being smooth to spiky might match the configuration of spherical harmonics better. From Figure 4, for the large k_s/k_d and/or large n, it is clear that the representation is not sufficient.

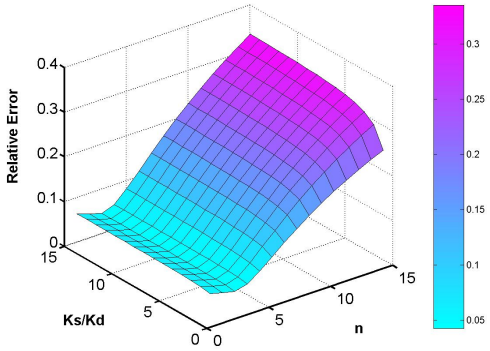

Figure 4. Representation error vs. k_s/k_d and n.

The topological geometries of Fourier coefficients for a_0, a_1, and b_1 are shown in Figure 5, where $k_s/k_d = 5$ and $n = 15$. Note that each coefficient of the same-order in the Fourier transform depends on directions, and we can decompose it into a smooth background and a peak. The height of peak is much larger in Figure 5(a), comparable to the smooth background in Figure 5(b), and opposite to the sign of smooth background in Figure 5(c). We will represent the smooth background with a linear combination of low-level spherical harmonics, and the sharp peak with a Gaussian function.

Note that we do not know the optimal critical angle to decompose the smooth background from sharp peak. Therefore, we calculate the relationship of the relative error versus the critical angle first, and then determine the critical angle corresponding to the minimal relative error. Figure 6 shows the relative error versus the critical angle. The incident direction is ($\theta_i = 15$, $\varphi_i = 0$) and the maximum level of spherical harmonics $L = 1$.

In Figure 6, the minimum relative errors are lower than 7% for all curves. For the same value of n, the critical angle for the minimum relative error does not change with the increase of k_s/k_d. However, for the same value of k_s/k_d, the error decreases with n. This is due to the fact that the increase in k_s/k_d only leads to an increase in the height of the peak relative to the smooth background, and does not change the width of peak. Therefore, the critical angle does not change with k_s/k_d. However, an increase in the Phong power causes a clear decrease of the width of the peak, and therefore the critical angle decreases with n.

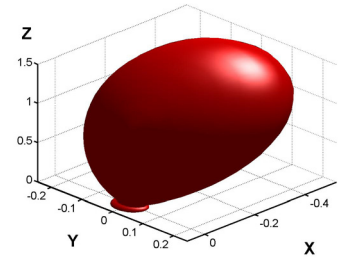

(a)

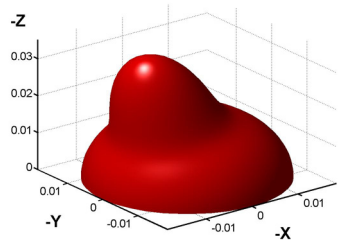

(b)

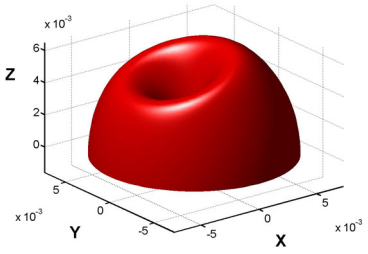

(c)

Figure 5. Geometry of Fourier coefficients, (a) for a_0, (b) for a_1, and (c) for b_1.

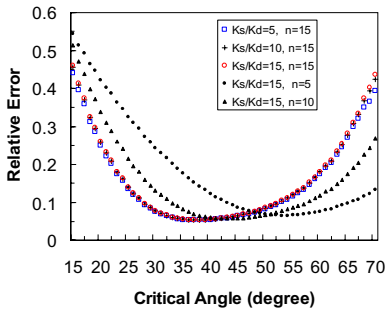

Figure 6. The relative errors of all the sampled outgoing directions vs. the critical angle.

Figure 7 shows the comparison of the represented spectral BRDFs with the originally generated data for $k_s/k_d = 15$ (see Figure 4). Here, the critical angle is 37 degrees, and the outgoing direction ($\theta_o = 15$, $\varphi_o = 180$) for Figure 7(a) gives the center position of the peak. The relative error is 0.048. The outgoing direction for Figure 7(b) is ($\theta_o = 15$, $\varphi_o = 135$), and the relative error is 0.025. The outgoing direction for Figure 7(c) is ($\theta_o = 15$, $\varphi_o = 90$), and the relative error is 0.028. Finally, the outgoing direction for 7(d) is ($\theta_o = 15$, $\varphi_o = 0$), and the relative error is 0.03. For all these outgoing directions, the reconstructed BRDFs using the parameters in our hybrid method agree well with the original BRDFs.

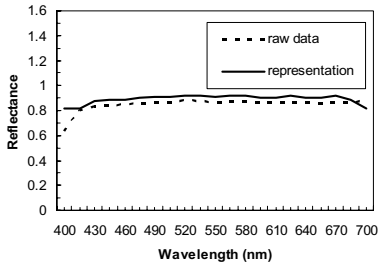

(a)

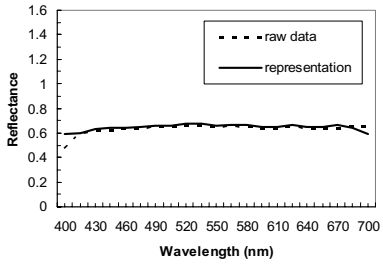

(b)

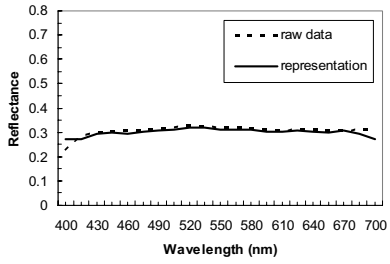

(c)

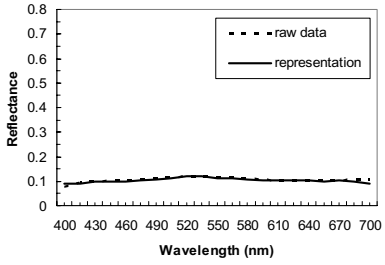

(d)

Figure 7. Comparison of the original (raw) BRDF and the reconstructed one using the proposed hybrid representation for different outgoing directions.

4. Conclusions

We have proposed a hybrid method to optimize the representation efficiency of spectral BRDFs. This method first performs a Fourier transform in the wavelength dimension, and then decomposes the Fourier coefficients into a smooth background and a sharp peak. The smooth background is represented with a linear combination of spherical harmonics and the peak with a Gaussian function.

We have studied the errors between the representation and the original spectral BRDFs (from the Phong model) versus a number of relevant parameters. Our results show that, for smooth spectral BRDFs, it is sufficient to represent spectral BRDFs directly using a linear combination of spherical harmonics up to level 4. However, for those spectral BRDFs with a sensitive dependency on the outgoing direction, it is important to decompose the Fourier coefficients into a smooth background and a sharp peak. The smooth background is represented with the linear combination of low-level spherical harmonics, and the sharp peak with a Gaussian function. Using the proposed hybrid method, a more compact representation is achieved.

As future work, it is interesting to test the hybrid method using spectral BRDFs obtained from measurements or simulations. The key idea of decomposition of the smooth background and sharp peak in a function can be easily extended to the case with multiple peaks (for example, spectral BRDFs involving diffraction usually have multiple peaks[2,27]). Finally, the hybrid method will be useful for spectrally-based image synthesis and analysis, as well as for the long-term data storage of spectral BRDFs.

References

1. A. S. Glassner, Principles of Digital Image Synthesis, Morgan Kaufmann, San Francisco, CA, 1995, pg. 664.
2. P. Beckmann and A. Spizzichino, The Scattering of Electromagnetic Waves from Rough Surfaces, MacMillan, New York, NY, 1963.
3. K. E. Torrance and E. M. Sparrow, J. Opt. Soc. Am., 57, 1105 (1967).
4. B. T. Phong, Comm. ACM, 18, 449 (1975).
5. J. F. Blinn, Computer Graphics, 11, 192 (1977).
6. R. L. Cook and K. E. Torrance, ACM Trans. Graph., 1, 7 (1982).
7. X. D. He, K. E. Torrance, F. X. Sillion, and D. P. Greenberg, Computer Graphics, 25, 195 (1991).
8. G. J. Ward, Computer Graphics, 26, 265 (1992).
9. Y. Sun, Self Shadowing and Local Illumination of Randomly Rough Surfaces, Proc. of Computer Vision and Pattern Recognition (CVPR), pg. 158. (2004).
10. B. Cabral, N. Max, and R. Springmeyer, Computer Graphics, 21, 273 (1987).
11. S. H. Westin, J. R. Arvo, and K. E. Torrance, Computer Graphics, 26, 255 (1992).
12. R. Ramamoorthi, and P. Hanrahan, An Efficient Representation for Irradiance Environment Maps, Proc. of SIGGRAPH, pg. 497. (2001).
13. R. Ng, R. Ramamoorhi, and P. Hanrahan, Triple Product Wavelet Integrals for All-Frequency Relighting, Proc. of SIGGRAPH, pg. 477. (2004).
14. P. Schröder and W. Sweldens, Computer Graphics, 29, 161 (1995).
15. P. Lalonde and A. Fournier, IEEE Transactions on Visualization and Computer Graphics, 3, 329 (1997).
16. J. Kautz, and M. D. McCool, Interactive rendering with arbitrary BRDFs using separable approximations, Proc. of the 10th EUROGRAPHICS Workshop on Rendering, pg. 281. (1999).
17. M. D. McCool, J. Ang, and A. Ahmad, Homomorphic Factorization of BRDFs for High-Performance Rendering, Proc. of SIGGRAPH, pg. 185. (2001).
18. F. Suykens, K. von Berge, A. Lagae, and P. Dutre, Interactive Rendering with Bi-directional Texture Functions, Computer Graphics Forum 22, 3, EUROGRAPHICS 2003.
19. J. Lawrence, S. Rusinkiewicz, and R. Ramamoorthi, Efficient BRDF Importance Sampling using a Factored Representation, Proc. of SIGGRAPH, pg. 496. (2004).
20. R. A. Hall, Illumination and Color in Computer Generated Imagery, Springer-Verlag, New York, NY, 1989.
21. M. S. Peercy, Linear Color Representations in Full Spectral Rendering, Proc. of SIGGRAPH, pg. 191. (1993).
22. J. S. Gondek, Gray W. Meyer, and J. G. Newman, Wavelength Dependent Reflection Functions, Proc. of SIGGRAPH, pg. 213. (1994).
23. Y. Sun, F. D. Fracchia, M. S. Drew, and T. W. Calvert, A Spectrum-Based Framework for Realistic Image Synthesis, The Visual Computer, 17, 429 (2001).
24. H. Xu, and Y. Sun, Representing Scattering Functions with Spherical Harmonics of Spectral Fourier Components, Computational Imaging II, Proc. of SPIE and IS&T Electronic Imaging, pg. 22. (2004).
25. H. Xu, Y. Tong, and Y. Sun, Composite Method for Efficient Data Representation, Proc. of IEEE EIT Conference, 2003.
26. J. D. Foley, A. V. Dam, S. K. Feiner, and J. F. Hughes, Computer Graphics Principles and Practice, Second Edition, Assison-Wesley, Massachusetts, 1996.
27. Y. Sun, F. D. Fracchia, M. S. Drew, and T. W. Calvert, Rendering Iridescent Colors of Optical Disks, Proc. of the 11th EUROGRAPHICS Workshop on Rendering, pg. 341. (2000).

Biographies

Huiying Xu received a Master degree in computer science and engineering in SUNY at Buffalo and a Ph.D in physics from the Institure of Physics, Chinese Academy of Sciences. His research interests include computer graphics, imaging, and visualization. He is researching on physically based illumination modeling and BRDF representation.

Yinlong Sun is an assistant professor in the Department of Computer Science and is directing Photometric Imaging Lab at Purdue University. His research interests include realistic image synthesis, scientific visualization, color science, biomedical imaging and computational neuroscience.